

# A Theoretical Investigation of the Electronic Structure and Spin Polarization in CrO<sub>2</sub>

Jon D. Swaim, Giuseppe Mallia and Nicholas M. Harrison

Department of Chemistry, Imperial College London, London SW7 2AZ United Kingdom

## ABSTRACT

The prospects for devices based on the manipulation of electronic spin rather than charge (spintronics) are based on the identification of materials which support strongly spin-polarized currents. The ferromagnetic material, CrO<sub>2</sub>, has found wide spread use in magnetic recording applications and, due to its theoretical 100% spin-polarization, has potential for use in spintronics. Previous band structure calculations predict CrO<sub>2</sub> to be a half-metallic ferromagnet, but the underlying electronic structure of CrO<sub>2</sub> is still controversial. In the current work strong electron-electron interactions are introduced using the hybrid-exchange approximation to DFT using the B3LYP and PBE0 functionals [1-2]. The computed electronic structure is found to be significantly different to that computed within the LDA and to be consistent with recent spectroscopy measurements. In particular there is an improved prediction of the energy gap in minority spin states due to the effects of strong *d-d* interactions.

**Keywords:** CrO<sub>2</sub>, spintronics, half-metal, ferromagnetism, hybrid, DFT

## 1 Introduction

CrO<sub>2</sub> has received much attention as a potential spintronic material due to theoretical predictions that it is a half-metallic ferromagnet [3-7]. Half-metallic ferromagnets are completely spin-polarized at the Fermi level ( $E_F$ ), with a metallic density of majority spin (spin-up) states and an insulating band gap in the minority (spin-down) states. Point-contact Andreev reflection spectroscopy and spin-polarized tunneling experiments have observed a spin-polarization of the conduction electrons that is larger than 95% [6]. CrO<sub>2</sub> therefore has potential for use as a source of spin-polarized electrons in magnetic tunneling applications such as magnetic random access memory [7]. CrO<sub>2</sub> is a room temperature ferromagnet with a Curie temperature,  $T_C$ , of 390 K [8] with the strong magnetic coupling thought to be due to double exchange interactions [9]. Although the transport properties are not yet well established, bulk CrO<sub>2</sub> is generally considered to be a poor metal, exhibiting a  $T^2$  dependence on resistivity above a characteristic

temperature between 80-100 K and, at low very  $T$ , a residual resistivity of  $5 \mu\Omega\text{cm}$  [10]. The  $T^2$  dependence is indicative of strong electron-electron interactions and its suppression at very low  $T$  has been assigned to the absence of minority-spin states (at  $E_F$ ) and thus the exclusion of spin flip scattering by magnon excitations [11].

CrO<sub>2</sub> crystallizes in the rutile structure (space group  $D_{4h}^{14}$ :  $P4_2/mnm$ ) with two formula units per unit cell. The Bravais lattice is tetragonal with lattice constants  $a = b = 4.421 \text{ \AA}$  and  $c = 2.916 \text{ \AA}$  [9]. Each Cr atom is surrounded by six O atoms, and the CrO<sub>6</sub> octahedron gives rise to a crystal field potential that removes the degeneracy of the Cr-3*d* orbitals, splitting them into a  $t_{2g}$  triplet ( $d_{xy}$ ,  $d_{yz}$  and  $d_{zx}$ ) and an  $e_g$  doublet ( $d_{x^2-y^2}$  and  $d_{z^2-r^2}$ ) [13].

The electronic structure of CrO<sub>2</sub> has been studied previously within DFT using several different approximations to electronic exchange and correlation. Schwarz first predicted CrO<sub>2</sub> to be a half-metallic ferromagnetic using the LDA in 1986 [3]. The LDA was seen to predict a finite density of states (DOS) at  $E_F$  for spin-up electrons and a gap of 1.5 eV in the spin-down spectrum. The inadequacies of the LDA and generalized gradient approximations (GGA) for studying strongly correlated systems are, however, well known [4]. One of the reasons is the unphysical self-interaction of electrons implicit in non-orbitally dependent effective potentials. In strongly correlated systems, this self-interaction can delocalize the 3*d* electrons, underestimate band gaps and incorrectly describe the ground state (e.g., metallic rather than insulating) [5]. We point out that a number of measurements, including x-ray absorption spectroscopy [7], resistivity [11] and optical [12], have suggested that strong correlation effects are present in CrO<sub>2</sub>. The LDA+ $U$  approach provides an *ad hoc* approach for approximating the electron-electron interactions by introducing an on-site Coulomb potential  $U$ . LDA+ $U$  band structure calculations by Korotin *et al.* yielded improved semi-quantitative agreement with the DOS measured by x-ray and ultraviolet photoemission experiments [13]. Recently, hybrid density functional methods such as B3LYP and PBE0 have been shown to be quite successful in the description of strongly correlated systems [14]. In these functionals, the non-local Hartree-Fock exchange is mixed with the GGA exchange-

correlation energy, reducing the self-interaction error and leading to improved estimates of band gaps [15], magnetic moments [16] and magnetic coupling constants [14]. In this paper we apply the B3LYP and PBE0 hybrid-exchange functionals to the half-metallic ferromagnet CrO<sub>2</sub>. In agreement with previous work [17], our results show that correlation effects beyond LDA are essential in understanding the electronic and magnetic properties of CrO<sub>2</sub>. We demonstrate that hybrid-exchange functionals can lead to improved prediction of band gaps and *d-d* correlation effects in CrO<sub>2</sub>.

## 2 Computational Details

All unrestricted Hartree-Fock (UHF) and density functional theory (DFT) calculations were performed using the CRYSTAL06 software [18]. For DFT calculations, the exchange-correlation energy was evaluated in the LDA, GGA as defined by Perdew, Burke and Ernzerhof (PBE), and B3LYP and PBE0 hybrid-exchange approximations. In the B3LYP method, the amount of exact Fock exchange mixed into the GGA exchange-correlation functional (20 %) was determined by fitting theoretical results to thermochemical data for certain atoms and molecules [16]. Interestingly, the functional has turned out to be quite successful in describing periodic systems. The PBE0 functional, developed by Perdew, Burke and Ernzerhof [19], is based on fourth-order perturbation theory and includes 25% Fock exchange.

All atoms are described as Bloch functions expanded with atom-centered Gaussians [18]. The Cr atom is represented with a 86-411G\* basis set (one *s*, four *sp*, and two *d* shells) adopted from a previous Cr<sub>2</sub>O<sub>3</sub> study [20]. The basis set for the O atom is a 8-411G\* contraction (one *s*, three *sp*, and one *d* shells) taken from an Al<sub>2</sub>O<sub>3</sub> study [21]. In the calculations, a shrinking factor of 8 was adopted to form a reciprocal mesh of *k*-points in the first Brillouin zone according to the Pack-Monkhorst method [18]. Thresholds of 10<sup>-7</sup>, 10<sup>-7</sup>, 10<sup>-7</sup>, 10<sup>-7</sup> and 10<sup>-14</sup> were used as tolerances for the mono-electronic and bi-electronic integrals, and the overall self-consistent field procedure was set to converge when  $\Delta E = 1 \times 10^{-7}$  Hartree. The cell parameters and internal coordinates were optimized using analytical energy gradients with respect to the cell vectors and nuclear coordinates, respectively.

## 3 Results & Discussion

In agreement with experimental work, the ground state energy of the ferromagnetic phase,  $E_{FM}$ , was always found to be lower than that of the antiferromagnetic phase,  $E_{AFM}$ . The relative stability of the phases is shown in Table 1 as the energy difference in the two phases,  $\Delta E = E_{AFM} - E_{FM}$ . In periodic UHF and DFT

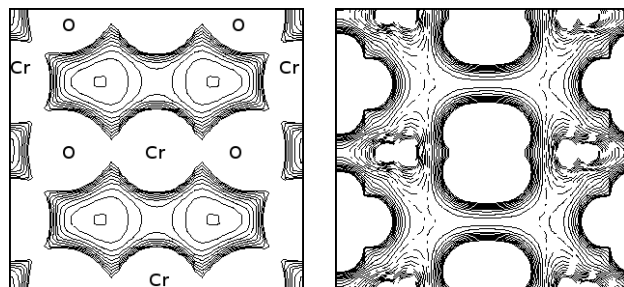


Figure 1: Total (left) and spin (right) density maps in 110 plane. Positive continuous and negative dashed lines represent spin-up and spin-down densities, respectively.

studies based on the Kohn-Sham formalism, the Slater determinants are not eigenfunctions of total square spin operator, but of  $\hat{S}_z$ , the *z* component of the spin operator. Hence, the magnetic coupling of two Cr<sup>4+</sup> cations each with total spin  $S=1$  is described by the Ising Hamiltonian

$$\hat{H}_{\text{Ising}} = - \sum_{i,j} J_{ij} \hat{S}_{iz} \cdot \hat{S}_{jz} \quad (1)$$

where  $\hat{S}_{iz}$  and  $\hat{S}_{jz}$  are the spin operators for sites *i* and *j*, respectively, and  $J_{ij} < 0$  corresponds to antiferromagnetic order. The extraction of *J* from the Ising Hamiltonian has been justified on the basis that particular eigenfunctions have equivalent expectation values for both the Heisenberg and Ising Hamiltonians, and thus a mapping exists between the model Hamiltonians [22]. However, in CrO<sub>2</sub>, only *Z* nearest neighbor magnetic ions are considered ( $Z = 8$  for CrO<sub>2</sub>), so the magnetic coupling constant *J* can be extracted from the relation  $\Delta E = JS^2Z$  [14]. An estimate of the Curie temperature  $T_C$  can then be obtained within the mean-field approximation:

$$T_C = \frac{S(S+1)}{3k_B} J \quad (2)$$

where  $k_B$  is Boltzmann's constant [23]. Values of *J* and  $T_C$  are listed in Table 1, as well as the net atomic charges *q* and spin moments  $\mu$  obtained from the Mulliken population analysis. Previous work has shown that hybrid-exchange functionals with 35% Fock exchange can lead to a proper description of magnetic coupling, but other functionals often overestimate *J* [14]. Indeed, our B3LYP magnetic coupling constant was overestimated by  $\sim 30\%$ . In the ferromagnetic case, all of the functionals produced Cr spin moments on the order of  $2 \mu_B$ . Fig. 1 shows the charge and spin density maps of the ferromagnetic ground state from the B3LYP calculation.

The calculated DOS from LDA and PBE are nearly identical, and indeed bear strong resemblance to those

Table 1: The energy difference  $\Delta E$  (eV) between FM and AFM phases relative to FM phase, magnetic coupling constant  $J$  (eV), mean-field Curie temperature (K), net atomic charges  $q = Z - (n_\alpha + n_\beta)$  ( $e$ ) and spin moments  $\mu = n_\alpha - n_\beta$  ( $\mu_B$ ).

	$\Delta E$	$J$	$T_C$	FM				AFM			
				$q$		$\mu$		$q$		$\mu^*$	
				Cr	O	Cr	O	Cr	O	Cr	O
LDA	0.348	0.044	340.412	1.926	-0.963	2.090	-0.045	1.910	-0.955	1.631	0.006
PBE	0.750	0.094	727.245	1.961	-0.981	2.175	-0.087	1.948	-0.974	1.699	0.010
B3LYP	0.523	0.065	502.882	2.058	-1.029	2.295	-0.148	2.065	-1.033	2.048	0.011
PBE0	0.331	0.041	317.202	2.075	-1.037	2.428	-0.214	2.101	-1.050	2.113	0.019
UHF	0.000			2.575	-1.287	2.151	-0.076	2.224	-1.112	2.957	0.528
Exp.			390-400								

\* Magnitudes of spin moments

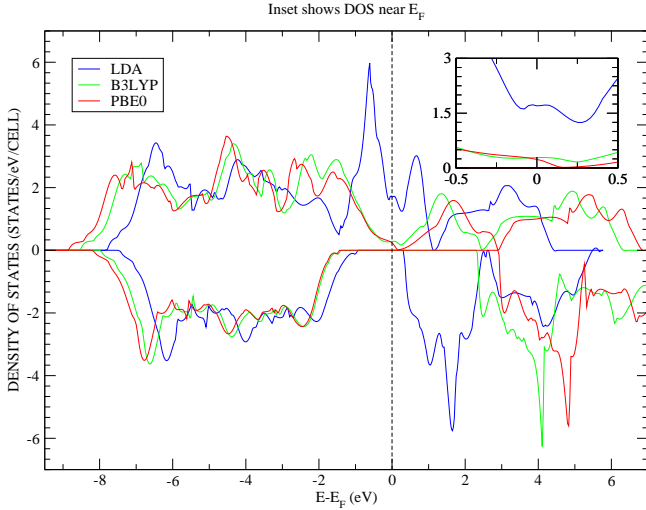


Figure 2: Spin-resolved DOS from LDA, B3LYP and PBE0 functionals. Inset shows DOS near  $E_F$ .

produced by previous authors. The notable exception is the fact that PBE predicts a slightly larger spin-down band gap (1.9 eV) than LDA (1.5 eV). To our knowledge, the only experimental study that has reported the size of this band gap is infrared spectroscopy work by Singley *et al.*, in which they ascribe a resonance of  $\omega = 270000\text{cm}^{-1} = 3.35$  eV to this gap [12]. As expected, both LDA and PBE calculations underestimate this band gap.

Our results show several important differences in the DOS between the hybrid-exchange and LDA-based functionals. We note that, unlike the previous LDA+ $U$  studies, B3LYP and PBE0 show the formation of a pseudogap near  $E_F$  in the spin-up electrons (Fig. 2). The small but finite DOS at  $E_F$  is in good qualitative agreement with recent photoelectron spectroscopy studies [8]. Moreover, the spin-down band gaps calculated within B3LYP (3.5 eV) and PBE0 (4.3 eV) are in much bet-

ter agreement with the experimental value than LDA or PBE. Our results agree quite well with the previous work [15] suggesting B3LYP to be an appropriate functional for estimating band gaps. However, all reported theoretical values to date are on the order of eV, and it remains unclear how the magnitude of this band gap relates to the temperature (80-100 K) at which spin-flip scattering is observed in the form of  $T^2$  resistivity dependence. Our band calculations do not fully include many-body correlation effects, so this difference in spin-flip energy will remain to be elucidated for now. However, in the spirit of realizing the potential of  $\text{CrO}_2$  as a spintronic material, the available states at  $E_F$  and their dependence on  $T$  must be investigated. Recently, Chioncel *et al.* have employed LDA with dynamical mean field theory (LDA+DMFT) as a means to address dynamical correlation effects. They have reported spin-down low-energy excitations at  $E_F$  in semi-quantitative agreement with spin-polarization measurements at similar temperatures [17].

Transition metal (TM) oxides can be classified in terms of the on-site  $d$ - $d$  Coulomb energy  $U$ ,  $p$ - $d$  charge transfer energy  $\Delta$  and the ligand  $p$ -metal  $d$  hybridization energy  $t$ , based on a scheme proposed by Zaanen, Sawatzky, and Allen (ZSA) [24]. The Coulomb energy  $U$  is defined as the energy required to remove an electron from a  $d$  orbital and place it in another  $d$  orbital site,  $U = E(d^{n+1}) + E(d^{n-1}) - 2E(d^n)$ , where hybridization is neglected, and  $E$  always represents the lowest multiplet configuration. The charge transfer energy  $\Delta$  is the energy required to excite a ligand  $p$  electron to a transition metal  $d$  orbital,  $\Delta = E(d^{n+1}\underline{L}) - E(d^n)$ , where  $L$  denotes a ligand hole. TM oxides are considered to be Mott-Hubbard insulators when  $U < \Delta$  and charge-transfer insulators when  $U > \Delta$ . In this formalism, we look to the partial Cr and O DOS for evidence of  $U$  and  $\Delta$  in the bulk electronic structure. In the calculated DOS from LDA and PBE, the Cr- $3d$  and

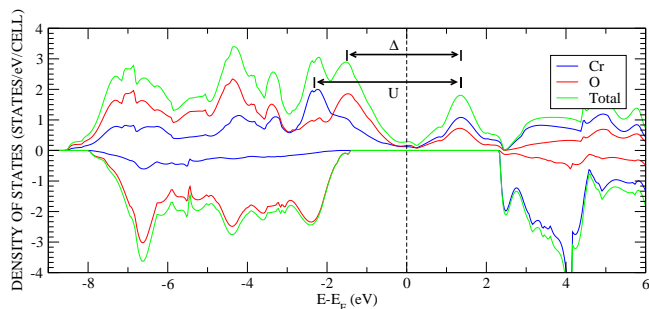


Figure 3: Partial Cr and O DOS from B3LYP.

O-2p peaks below  $E_F$  occur at the same energy, i.e.,  $U \simeq \Delta$ , which places  $\text{CrO}_2$  on the border on the Mott-Hubbard and charge-transfer regimes, similar to antiferromagnetic  $\text{Cr}_2\text{O}_3$ . However, the hybrid-exchange functionals produce results in which  $U > \Delta$ , supporting the work by Korotin *et al.* with the classification of  $\text{CrO}_2$  as a charge-transfer insulator. Qualitative estimates of  $U$  (and  $\Delta$ ) are defined as the energy gaps between the Cr-3d (O-2p) peak below  $E_F$  and the Cr-3d peak above  $E_F$  (Fig. 3). We also wish to point out that B3LYP places the Cr-3d peak at 2.3 eV below  $E_F$ , in excellent agreement with recent photoelectron spectroscopy data by Ventrice *et al.* [8].

The classification of  $\text{CrO}_2$  as a charge-transfer insulator is supported by the B3LYP and PBE0 band structures, in which one of the bands crossing  $E_F$  is of pure O-2p character. As expected, the band structure from B3LYP (shown in Fig. 4) and PBE0 are typical of a half-metallic ferromagnetic in that they appear 100% spin-polarized with a metallic density of spin-up states at  $E_F$ . The hybrid functionals predict more Cr-3d-O-2p hybridization than LDA or PBE, consistent with LDA+ $U$  results that led authors to conclude that the ground state of  $\text{CrO}_2$  is ferromagnetic through the double exchange mechanism [13].

## 4 Conclusions

The electronic structure of bulk  $\text{CrO}_2$  was investigated using hybrid-exchange density functional theory. We showed that the hybrid-exchange functionals give better theoretical predictions of the energy gap in the minority-spin states and an improved description of strong electron-electron interactions. We emphasize that future theoretical methods should include an accurate treatment of electron-correlation effects in order to properly understand the nature of  $\text{CrO}_2$ .

## REFERENCES

- [1] A. D. Becke, *J. Chem. Phys.*, **98**, 5648 (1993)
- [2] C. Adamo and V. Barone, *J. Chem. Phys.* **110**, 6158 (1999)

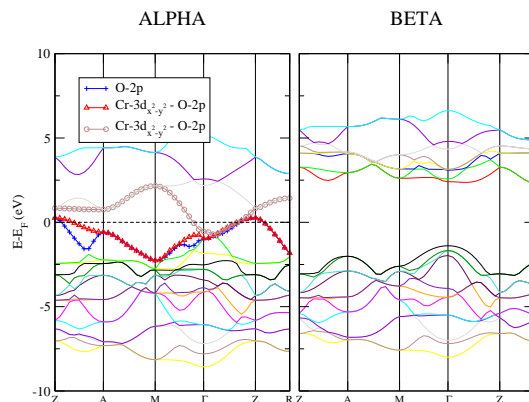


Figure 4: Calculated band structure from B3LYP.

- [3] K. Schwarz, *J. Phys. F: Met. Phys.*, **16** L211-L215 (1986)
- [4] Perdew *et al.*, *Rev. Rev. B.*, **23**, 5048-5079 (1981)
- [5] W. E. Pickett, *Rev. Mod. Phys.*, **61**, 433 (1989)
- [6] Soulen *et al.*, *Science*, **282**, 85-88 (1998)
- [7] C. B. Stagarescu *et al.*, *Phys. Rev. B*, **61** 14, R9233-R9236 (2000)
- [8] C. A. Ventrice *et al.*, *J. Phys.: Condens. Matter* **19** 315207 (2007)
- [9] P. Schottmann, *Phys. Rev. B* **67** 174419 (2003)
- [10] S. M. Watts *et al.*, *Phys. Rev. B* **61** 14 9621-9626 (2000)
- [11] K. Suzuki and P. M. Tedrow, *Phys. Rev. B*, **58**, 17 11597-11602 (1998)
- [12] E. J. Singley *et al.*, *Phys. Rev. B*, **60**, 6 4126-4130 (1999)
- [13] Korotin *et al.*, *Phys. Rev. Lett.* **80**, 19 4305-4308 (1998)
- [14] X. B. Feng and N. M. Harrison, *Phys. Rev. B*, **70**, 092402 (2004)
- [15] Muscat *et al.* *Chem. Phys. Lett.* **342**, 3-4 397-401 (2001)
- [16] X. B. Feng, *Phys. Rev. B*, **69**, 155107 (2004)
- [17] Chioncel *et al.* *Phys. Rev. B* **75**, 140406(R) (2007)
- [18] V. R. Saunders *et al.*, CRYSTAL06 Users Manual, Universit di Torino, Torino, 2006.
- [19] J. P. Perdew *et al.* *Journal Chem. Phys.* **105**, 12 9982-9985 (1996)
- [20] M. Catti *et al.* *J. Phys. Chem. Solids* **57**, 1735-1741 (1996)
- [21] M. Catti *et al.* *Phys. Rev. B* **49**, 14179 (1994)
- [22] I. de P.R. Moreira and F. Illas, *Phys. Rev. B*, **55** 7, 4129-4136 (1997)
- [23] N.W. Ashcroft and N.D. Mermin, *Solid State Physics*, Holt, Rinehart, and Winston, New York (1976)
- [24] Bocquet *et al.* *Phys. Rev. B* **53**, 3 1161-1169 (1996)